We are IntechOpen, the world's leading publisher of Open Access books Built by scientists, for scientists

4,800
Open access books available

122,000
International authors and editors

135M
Downloads

Our authors are among the

154
Countries delivered to

TOP 1%
most cited scientists

12.2%
Contributors from top 500 universities

CLARIVATE ANALYTICS BOOK CITATION INDEX INDEXED

WEB OF SCIENCE™

Selection of our books indexed in the Book Citation Index in Web of Science™ Core Collection (BKCI)

Interested in publishing with us?
Contact book.department@intechopen.com

Numbers displayed above are based on latest data collected.
For more information visit www.intechopen.com

Chapter 12

End-To-End Monitoring System for the Preventing Deterioration in Art and Cultural Objects

Luca Bencini and Stefano Maddio

Additional information is available at the end of the chapter

http://dx.doi.org/10.5772/48303

1. Introduction

A fundamental responsibility of a museum is the prevention of deterioration of art and artifacts through control of the environment in storage and exhibition. Preventive conservation entails storing, displaying, handling and maintaining a museum's collections in ways that promote long term stability and do not lead to deterioration. Thus, preventive conservation activities include monitoring the principal causes of deterioration, developing methods for secure display and storage, and ensuring the safety of works of art during their transport and loan to other museums.

Different types of collections need different forms of care. Many objects are composed of more than one material, each of which may respond differently to a variety of environmental factors. The major factors of deterioration are *light*, *temperature & humidity* and *pollutants*. Light is a form of energy that generates heat. Artifact deterioration is a result of chemical reactions that occur when an energy source changes the chemical structure of the object's surface. The amount of energy given off by a light source can be illustrated in the light spectrum. The electromagnetic spectrum is divided into wavelengths of energy, which range from low (radio waves) to high (gamma rays). The range of wavelengths from light sources (daylight and artificial light) can be divided into three regions: ultraviolet radiation or UV (300-400 *nm*), visible radiation (400-760 *nm*) and infrared radiation (over 760 *nm*). In essence, the shorter the wavelength of the light source, the more damaging to the surface of an object.

Temperature has a great effect on *Relative Humidity* (RH). Relative Humidity is a measure of the amount of moisture in the air relative to the amount the air is capable of holding, expressed as a percentage. If the air at a particular temperature contains half the water vapor it can hold at that temperature, the relative humidity is 50%. Acute changes in temperature and humidity will cause swelling and contraction as the materials in an object or artifact attempt to adjust to the environment. Objects are often composed of more than one type of material. Each material responds differently to water vapor in the air and adjusts to its particular *Equilibrium Moisture Content* (EMC) at different relative humidities. Of particular concern are the internal stresses

created by expansion and contraction of the different materials as moisture diffuses into or out of the surrounding air.

Pollutants work in combination with other factors, such as temperature, relative humidity (RH) and light to cause deterioration. The museum environment poses a particular challenge because objects are often exhibited or stored in microenvironments, such as display cases or storage units. If the enclosure were made of a pollution emitting material, it would create a microenvironment in which the pollutants would remain confined with the objects.

Finally, the packing of art objects for shipment is another important aspect of preventive care for both stable and unstable objects. The extent of handling involved in packing the artwork, crating the artwork, movement during travel, and then unpacking the artwork could cause physical and chemical damage.

The most suitable technology to fit an invasive method of monitoring the environment without man attendance is a Wireless Sensor Network (WSN) system [1], [2], [5], [3], [4].

The requirements that adopting a WSN are expected to satisfy in effective cultural heritage monitoring concern both *system level* issues (i.e., unattended operation, maximum network life time, adaptability or even self-reconfigurability of functionalities and protocols) and *final user* needs (i.e., communication reliability and robustness, user friendly, versatile and powerful graphical user interfaces). The most relevant mainly concerns the supply of *stand-alone* operations. To this end, the system must be able to run unattended for a long period also in the absence of electricity. This calls for an optimal energy management ensuring that the energy spent is directly related to the amount of traffic handled and not to the overall working time. An additional requirement is *robust operative conditions*, which needs fault management since a node may fail for several reasons. Other important properties are *scalability* and *adaptability* of the network's topology, in terms of the number of nodes and their density in unexpected events with a higher degree of responsiveness and reconfigurability. Finally, several user-oriented attributes, including *fairness*, *latency*, *throughput* and enhanced data querying schemes [6] need to be taken into account even if they could be considered secondary with respect to our application purposes because the WSN's cost/performance trade-off.

Taking the before mentioned user and system requirements into account, a monitoring system based on WSN technology was developed. As Fig. 1 shows, it is comprised of:

- an *one level cluster tree WSN* endowed with sensing capabilities;
- an *Ethernet* or a *GPRS Gateway* (cluster head) for each cluster to gather data and provide a TCP-IP based connection toward a *Remote Server*;
- a *web application* which manages information and makes the final user capable of monitoring and interacting with the instrumented environment.

A cluster tree topology was adopted because it is the network architecture that best suits the structure of a museum. Moreover it allows to obtain simplicity, better performance in terms of latency, scalability and isolation of devices.

A GPRS Gateway was realized to extend the area of applicability of the WSN to zones in absence of wired connections such as outdoor environments.

More details of hardware, software and communication protocol design are provided in the next sections. In particular the chapter is organized as follows. Sections 2, 3 and 4 deal

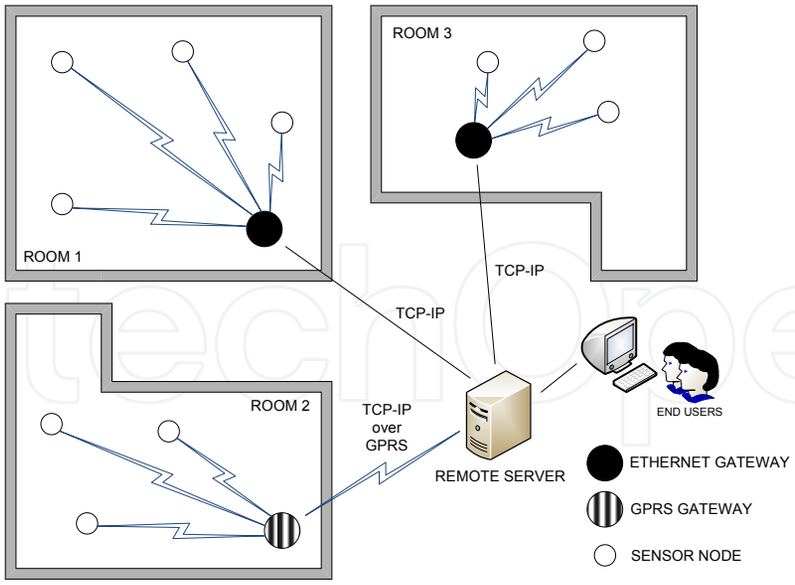

Figure 1. End-to-end WSN system

respectively with the system in terms of hardware, protocol and end user interface design. Section 2.3 is dedicated to a detailed description of the design of directional antennas. Section 5 describes the actual experiences, focusing on some case study analyses for highlighting the effectiveness and accurateness of the developed system. Finally, in Section 6 some conclusions are drawn in order to explain the future direction of the current research study.

2. Hardware and software design

Focusing on an end-to-end WSN system architecture, every constitutive element has to be selected according to the application requirements and scenario issues, especially the hardware platform. Many details have to be considered, involving the energetic consumption of the sensor readings, the power-on and power-save states management and a good trade-off between the maximum radio coverage and the transmitted power.

In the next subsections a detailed hardware description of the WSN components is provided.

2.1. Sensor node design

In order to allow greater flexibility in the placement of the network devices, each sensor node was realized separating the sensor unit (*Sensor Board*) from the power board and the communication unit (*Main Board*).

The Sensor Board is responsible for data acquisitions. As Fig. 2(a) shows, it can manage simultaneously two digital temperature-moisture sensors, one analogical light sensor, three analogical gas sensors (O_3, NO_2, SO_2) and one accelerometer-gyroscope sensor that is hardwired to the Sensor Board by a RS232 serial port. The Sensor Board recognizes automatically the sensors once they are plugged and sends Transducer Electronic Datasheets (TEDS) through the network up to the server, making an automatic sensor recognition possible by the system.

Table 1 provides a list of the sensor typologies used in our tests and applications.

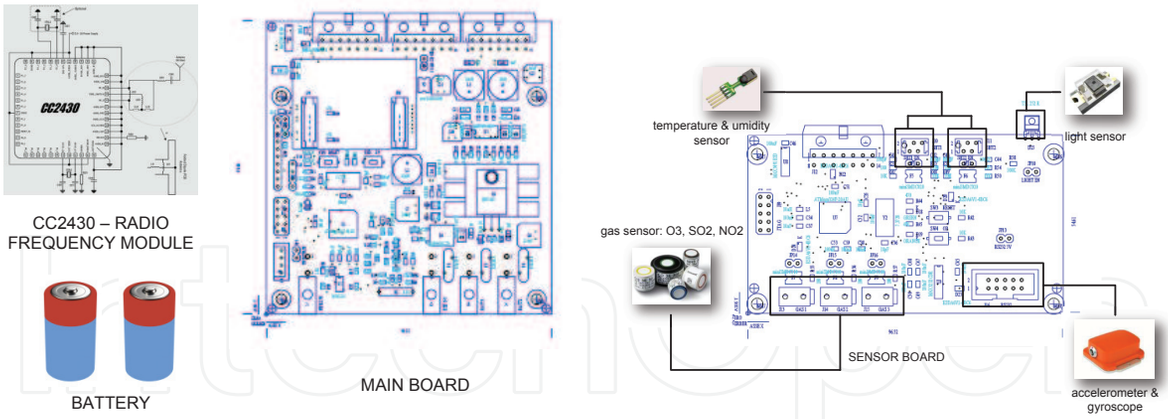

(a) Sensor Board (b) Main Board

Figure 2. Sensor Node

MANUFACTURER	MONITORED PARAMETER
SENSIRION - SHT75 [7]	Humidity & Temperature
MicroSemi - TAOS TSL252R-LF [8]	Light
City Tech - EZT3NDH [9]	NO_2
City Tech - EZT3SH [9]	SO_2
City Tech - O33E1F [9]	O_3
XSens - Mti [10]	Accelerometer & Gyroscope

Table 1. Sensor Typologies

The Main Board handles the communication with the Sensor Board and with the gateway and manages the charge and discharge of the batteries. As Fig. 2(b) shows, it is composed by a RF module equipped by a omnidirectional antenna, a master board and a power board. The power board includes ten 3200 mAh @ 1.8 V rechargeable batteries connected in series.

Some pieces of information about the power consumption and the lifetime of the sensor nodes are provided in Section 3 where the communication protocol is described.

The Main Board can support and manage up to a maximum of three Sensor Boards thanks to a RS422 serial bus.

The "core" of each sensor node resides in the software/firmware modules developed within the chips of the master board (*ATMEL ATmega644P microcontroller*), RF board (*Texas Instruments CC2430 System-On-Chip*) and Sensor Board (*ATMEL ATmega644P microcontroller*). In fact these C/assembler modules permits to manage high and low power states and the charge and discharge of the batteries, to realize finite state machines, to query sensors at fixed intervals and to achieve anti-blocking procedures in the case of software failures or deadlocks. An important role is played by the communication module that allows the information exchange between each node and the gateway.

2.2. Ethernet and GPRS Gateway

The Ethernet Gateway is a Main Board hardwired with an *AK-NORD XT-Nano ethernet module* [11] through a RS232 serial interface.

It is equipped by a 2.4 *GHz* switched beam antenna (see Section 2.3) and by ten 3200 *mAh* @ 1.8 *V* rechargeable batteries connected in series that provide emergency power for 212 hours when the input power source, the utility mains or the *Power over Ethernet* (PoE), fails.

Data between the Ethernet Gateway and Remote Server are carried out over TCP-IP communication and encapsulated in a custom protocol; from both local and remote interfaces it is also possible to access part of the Gateway's configuration settings. To avoid data lost caused by link failures, a 128 *KB* SRAM memory is also mounted on the board to allows for data buffering.

The GPRS embedded Gateway is a stand-alone communication platform designed to provide transparent, bi-directional wireless TCP-IP connectivity for remote monitoring. In conjunction with *Remote Data Acquisition* (RDA) equipment, such as WSN, it acts when connected with a sensor node or when directly connected to sensors and transducers.

The main hardware components that characterize the gateway are:

- a 2.4 *GHz* switched beam antenna (see Section 2.3);
- a miniaturized GSM/GPRS modem, with embedded TCP/IP stack [14] [16];
- a powerful 50 *MHz* clock microcontroller responsible for coordinating the bidirectional data exchange between the modem and the master node to handle communication with the Remote Server;
- an additional 128 *KB* SRAM memory added in order to allow for data buffering, even if the wide area link is lost;
- several A/D channels available for connecting additional analog sensors and a battery voltage monitor.

Since there is usually no access to a power supply infrastructure, the hardware design has also been oriented to implement low power operating modalities, using a 12 *Ah* @ 12 *V* rechargeable lead battery and in addition a 20 *W* solar panel when the gateway is deployed in outdoor environment.

Data between the GPRS Gateway and Protocol Handler are carried out over TCP-IP communication and encapsulated in a custom protocol; from both local and remote interfaces it is also possible to access part of the Gateway's configuration settings. The low-level firmware implementation of communication protocol also focuses on facing wide area link failures. Since the gateway is always connected with the Remote Server, preliminary connectivity experiments demonstrated a number of possible inconveniences, most of them involving the *Service Provider Access Point Name* (APN) and *Gateway GPRS Support Node* (GGSN) subsystems. In order to deal with these drawbacks, custom procedures called *Dynamic Session Re-negotiation* (DSR) and *Forced Session Renegotiation* (FSR), were implemented both on the gateway and on the CMS server. This led to a significant improvement in terms of disconnection periods and packet loss rates.

The DSR procedure consists in a periodical bi-directional control packet exchange, aimed at verifying the status of uplink and downlink channels on both sides (gateway and CMS). This approach makes facing potential deadlocks possible if there is asymmetric socket failure, which is when one device (acting as client or server) can correctly deliver data packets on the

TCP/IP connection but is unable to receive any. Once this event occurs (it has been observed during long GPRS client connections, and is probably due to Service Provider Access Point failures), the DSR procedure makes the client unit to restart the TCP socket connection with the CMS.

Instead, the FSR procedure is operated on the server side when no data or service packets are received from a gateway unit and a fixed timeout elapses: in this case, the CMS closes the TCP socket with that unit and waits for a new reconnection. On the other side, the gateway unit should catch the close event exception and start a recovery procedure, after which a new connection is re-established. If the close event should not be signaled to the gateway (for example, the FSR procedure is started during an asymmetric socket failure), the gateway would anyway enter the DSR recovery procedure.

In any case, once the link is lost, the gateway unit tries to reconnect with the CMS until a connection is re-established.

2.3. Antenna design

The typical basic antenna equipped in the sensor nodes of a WSN are *omnidirectional*, either in the form of printed IFA or as compact stylus. In this context, the term omnidirectional refers to a 2D isotropic behavior, as the canonical dipole antenna, radiating almost uniformly only in a transverse plane and affected by strong transmission zeros above and below. This kind of antenna is suitable for a isotropic broadcast communication (Figure 3(a)).

A *directional* antenna is a radiator specifically designed to be *directive* (Figure 3(b)). Directive antennas privilege the electromagnetic link toward specific direction, showing an high transmission gain peak. Directive antennas can improve the performance of WSNs in several ways. With a directional antenna the same received power is obtained with less transmitted power, achieving a better power efficiency - unicast communication. Alternatively, greater transmission range are possible with the same available power. With limited angular coverture, it operates as a spatial filter, which is an aid to contrast the interferences in a electrically polluted are, with significative advantages in term of link quality. Finally, the spatial re-usability can increase communication capacity and throughput. Nevertheless, a single antenna cannot be suitable for both broadcast and unicast links.

A *Switched Beam Antenna* (SBA) is a smart antenna able to establish a set of predetermined directional beams. An SBA is composed of a set of elementary radiators combined with a selection logic driven by a digital control activated by the node intelligence. While limited by the available sectors, switched beam antenna are simpler and cheaper than adaptive beamformers - antenna array able to generate beam in arbitrary direction - while maintaining similar advantages. The simplest SBA is made by a Single Pole N Through (SPNT) RF switch directly connected to an array of N printed antennas, whose geometry is arranged in order to cover the entire domain of interest.

Printed (patch) antennas are the most suitable radiators for SBA. Compatible to the standard PCB photo-etching technology and materials, at the price of a little performance drop, patches can assume any arbitrary planar shape, making them very versatile in terms of nominal resonant frequency, bandwidth, polarization and pattern shaping. When operating in fundamental mode, they typically exhibit a mono-lobe radiation pattern characterized by

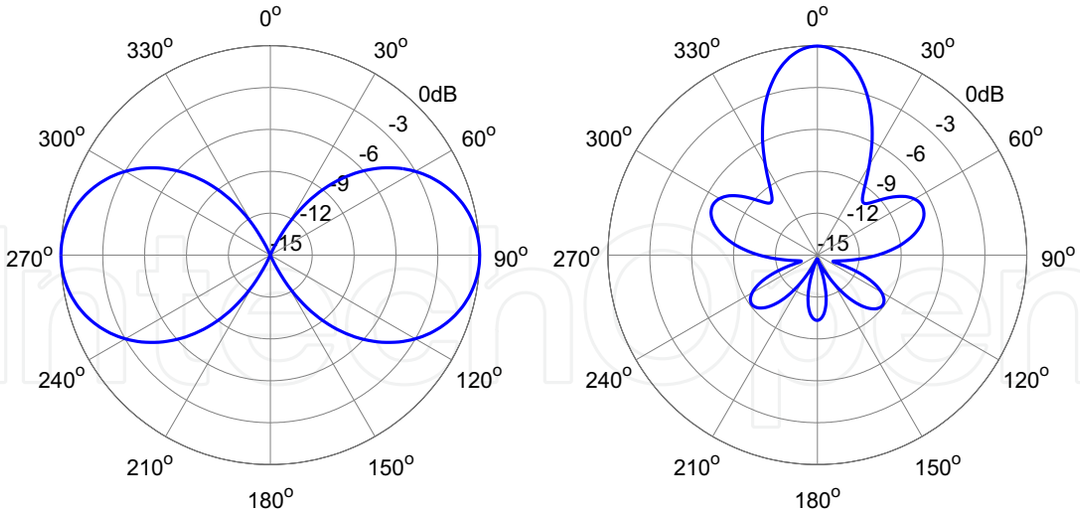

(a) Omnidirectional Pattern - Broadcast (b) Directional Pattern - Unicast

Figure 3. Typical Antenna Patterns

a radiation peak in the normal direction of the antenna plane (broadside radiator) with a maximum directivity in the range of 4-7 dB.

The SBA employed in the described WSN is a *Four Switched Beam Antenna* (FSBA), a device composed of four coaxially fed antennas arranged in a cubic structure as shown in Figure 6. The resulting elementary antenna layout designed in common FR4 substrate ($\epsilon_r = 4.4$, $h = 1.6$ mm, $\sigma_{Cu} = 5.8\,mS$) and its dimensions, along with the prototype photograph, are shown in Figure 4(b) Each antenna element ground is shaped in a $65\,mm \times 65\,mm$ square. The radiative system, while bulky, can operates as a mechanical shelter of the senor node.

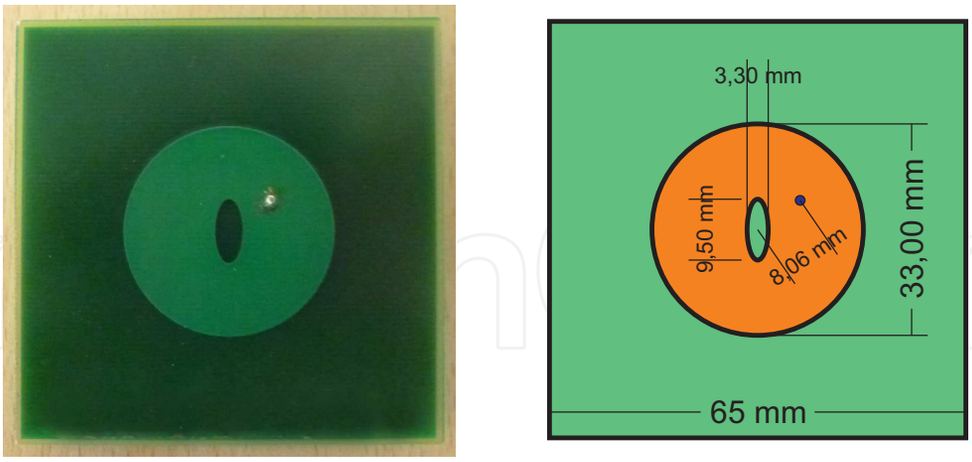

(a) Element Photograph (b) Element Layout With Quotes

Figure 4. Design and Photograph of the Elementary Antenna of the SBA

The antenna element of the proposed system are compact directive patch antennas operating in Circular Polarization (CP), which ensure communication regardless of relative orientation. CP is also as an effective aid to combat the multipath effect, since the radiated field by a LHCP antenna inverts its rotation sense after reflecting on the ground, becoming a RHCP field, thus

virtually invisible to a co-polarized LHCP receiving antenna. The Antenna design is based on the modal degeneration phenomenon, a smart way to achieve and control the CP effect without the aid of an external splitter. Following this approach, compact directive antenna design is possible [12, 13].

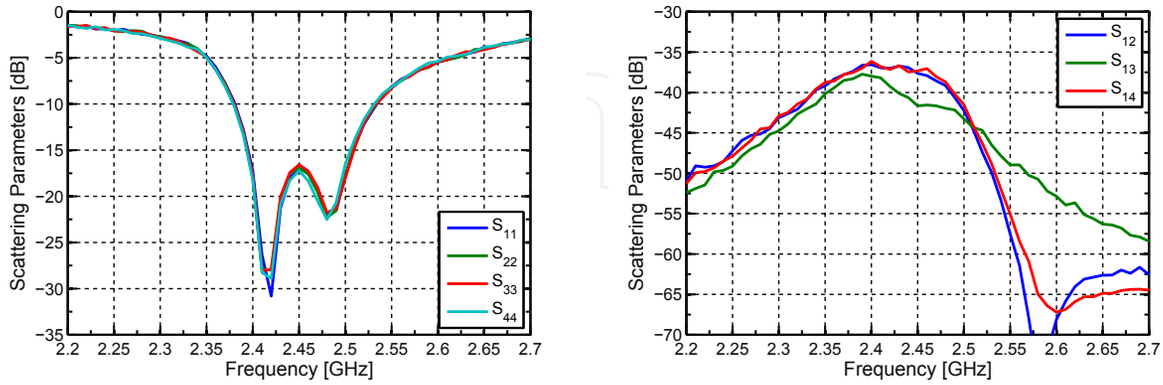

(a) Reflection Coefficient (S_{xx}) (b) Isolation (S_{xy})

Figure 5. Scattering Parameters of the Antenna Elements

Figure 5 shows the performance of the four antennas. The reflection coefficients are plotted in Figure 5(a), where a minimum around the center of ISM frequency confirms a good matching, quantified in a Return Loss (RL) of 17 dB and a 10 dB RL bandwidth exceeding 150 MHz. All the four traces exhibit the same dual min-max-min behaviour around the central frequency, a hint of the archived circular polarization in the area between the minimums. Dimensions and performance were traded off so as to be compact but at the same time without sacrificing performance. Figure 5(b) shows the isolation of the four antennas, confirming a minimum value of 36 dB, suitable for the application in exam.

The assembled structure composed of the four antennas shows a set of 4 individual directive pattern with a maximum over the four cardinal direction, individuated by the side of the box structure, and an Half Power Beam Angle of almost 90 degrees. The latter characteristic grants that the *cumulative pattern*, the pattern composed by the maximum of the four antennas, is almost isotropic, ensuring the communication coverture the entire 2π radian domain. The measurements azimuthal pattern at the design frequency of 2.45 GHz reveals a good Left Hand with a Co/Cross discrimination between 18 and 21 dB depending on the antenna. Optimal CP is achieved in the broad-side direction, while the back lobe experiments a CP inversion, a typical behavior of the modal degenerated antenna, which is an aid for the link discrimination. The absolute gain value is estimated as 3.85 dB, with an estimated antenna efficiency of, compatible with the sub-optimal performance of the cheap substrate.

In Figure 6 is depicted a Four Beam Antenna (FBA), proposed as the basic node of the WSN. The four sector beams of the 4BA are also shown. The radiation patterns are measured in operative condition, with the antenna elements connected to the switch. The maximum gain is estimated as 2 dB, a low value affected by the switch insertion loss and unavoidable co-channel coupling. The advantages in generating 4 beams is that the cumulative pattern can cover the entire 2D angular range with a cubic box arrangement, but dedicated links can be established toward the four directions.

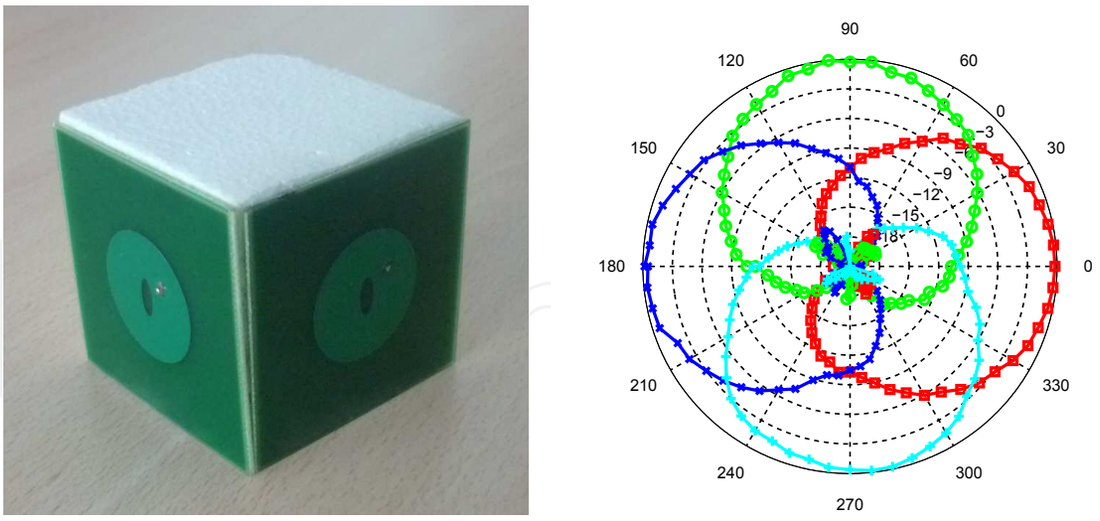

(a) Antenna Arrangement (b) Antenna Beams

Figure 6. Four Switched Beam Antenna Photograph and Radiative Performance

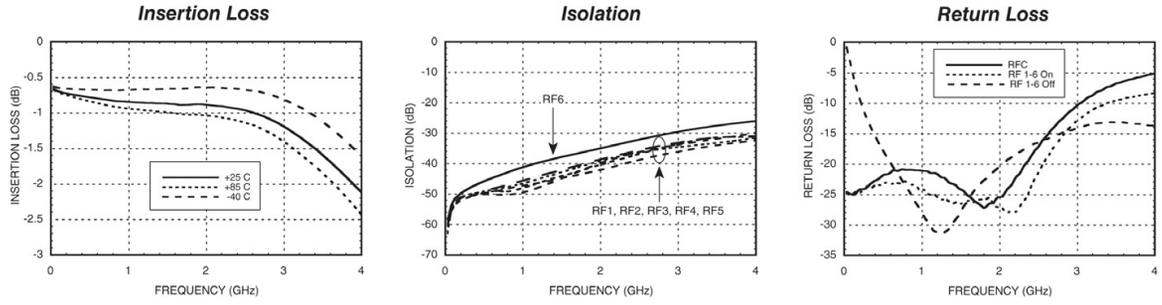

Figure 7. SP4T Characteristics Taken from Hittite Datasheet

The selection mechanism of proposed SBA is a non-reflective SP4T switch by Hittite, model HMC252QS24. The switch performance, reported in Figure 7, are suitable for the application in exam. The adoption of this kind of switch minimizes the coupling between the 4 radio channels ensuring a minimal pattern and polarization corruption.

3. Communication protocol design

Apart the Ethernet Gateway, all devices are energy constrained. Therefore smart power saving procedures have to be adopted to increase network lifetime. Some common approaches are the management of both sleep and active states, the on board integration of directional antennas and their integration within the communications framework. As these aspects belong to both the Physical (PHY) and Medium Access Control (MAC) layers, they might be integrated to achieve an overall energy efficiency, managing, for example, at the same time the duty cycle and the beams of the on board directional antennas. The way to accomplish this goal effectively relies on the so called *cross-layer* protocol design principle [15].

According to this principle, the communication protocol was designed and realized.

In the following sections the protocol stack is described and its performance are provided.

3.1. Physical and MAC layer

The Physical (PHY) layer and in part the Medium Access Control (MAC) layer are hardware implemented by the *Texas Instruments CC2430 System-On-Chip* in accordance with IEEE 802.15.4 standard [17].

The Physical layer (PHY) provides the data transmission service and performs channel selection and energy and signal management functions. It operates on 2400 - 2483.5 *MHz* unlicensed frequency bands with a rate of 250 *Kbps*. Moreover, it employs a 16 - ary quasi-orthogonal modulation technique, in which each four information bits are mapped into a 32 - chip pseudo-random noise (PN) sequence. The PN sequences for successive data symbols are then concatenated and modulated onto the carrier using an Offset Quadrature Phase Shift Keying (O-QPSK).

The Medium Access Control (MAC) layer implemented by the *Texas Instruments CC2430 System-On-Chip* allows the transmission of MAC frames through the use of the physical channel. Besides the data service, it also controls frame validation, guarantees time slots and offers hook points for secure services. Finally it implements CSMA-CA mechanism for channel access.

To improve the energy efficient of the system, a MAC protocol based on *sleep* and *active* states [18] [19] and IEEE 802.15.4 features and able to manage switched beam antennas was developed.

According to it, each device wakes up independently, entering an initial idle state (*init state*) in which it remains for the time interval necessary for performing the elementary CPU operations and to be completely switched on (T_{init}). Moreover, before entering the *discovery state*, each device starts to organize the time into frames whose durations areT_f .

In the *discovery state* each sensor node tries to associate itself with a gateway and to establish a time synchronization with it. Vice versa each gateway tries to build up its cluster of sensor nodes.

Each gateway remains in a listening mode for a time interval equal to $T_{set-up} \geq 2T_f$ and begins to periodically broadcast a HELLO message to each angular sector (i.e., the coverage area within a certain side lobe) sending its *ID* and its *phase*. The *phase* is the time interval after which the sender exits from the *discovery state*, enters the *regime state* and changes back in listening mode in that particular sector.

A sensor node that receives a HELLO message from a gateway adds it to the list of its own active gateways and transmits an acknowledgement. At the end of the *discovery state*, each sensor node chooses only one gateway as cluster head. Even so it keeps trace of the others for backup.

A gateway that receives a HELLO message from another gateway discards instead the information.

Each sensor node performs the same procedure. Since it is equipped by an omnidirectional antenna (dipole antenna), it has not to worry about changing the antenna's angular sector.

A sensor node that receives a HELLO message from another sensor node discards the information. A gateway that receives a HELLO message from a sensor node adds it to the list of its own active sensor nodes.

Once the *discovery state* has expired, each device enters the *regime state*. Within this state the operation mode is duty cycled with a periodic alternation of listening and sleeping sub-periods whose time intervals are T_l and T_s respectively. The duty cycle function is given by the following formula:

$$d = \frac{T_l}{T_l + T_s} \tag{1}$$

In the *regime state* each device tries to preserve the synchronization established during the *discovery state*. To this purpose each gateway sends a frame-by-frame HELLO message in a unicast way to the sensor nodes in its list belonged to different sectors according to the phase transmitted by them in previous HELLO messages. The same procedure is performed by each sensor node toward the gateway each one is associated with. Fig. 8 shows the synchronization messages exchange.

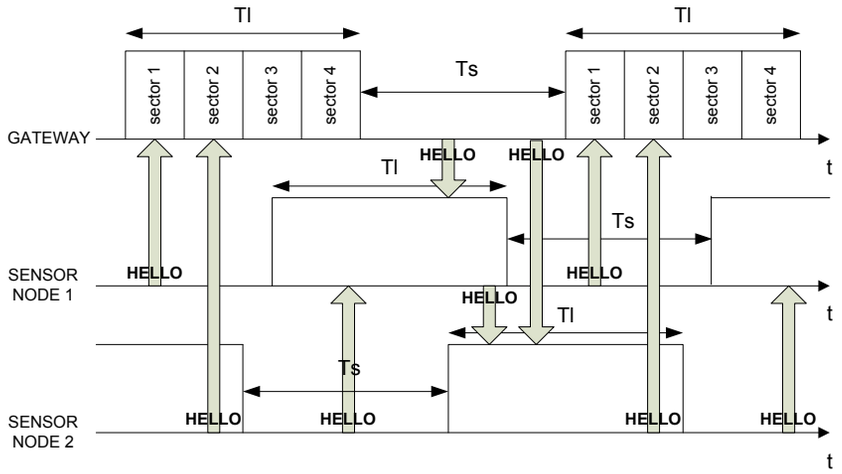

Figure 8. MAC Protocol Synchronization Messages Exchange

As in the *discovery state*, the HELLO message contains the *ID* and the *phase* that, in this case, is the time interval after which the sender claims to be again in the listening status waiting for the HELLO messages. The *phase* ϕ is evaluated according to the following rule:

$$\phi_1 = \tau - T_l \tag{2}$$

if the node is in the sleeping mode, where τ is the time remaining to the beginning of the next frame. Conversely, if the node is in the listening status, ϕ is computed as:

$$\phi_2 = \tau + T_s \tag{3}$$

To complete the protocol characterization, a device turns off entering the *off state* when its battery is depleted.

If a gateway presents an improper functioning or its battery is depleted, the sensor nodes belonging to its cluster are not capable of sending data to the Remote Server. To this purpose, a *recovery state* was introduced.

Each sensor node monitors every frame the *link quality* (LQ) defined as:

$$LQ = \frac{N_{Rx-GW}}{N_{Tx-SN}} \tag{4}$$

where N_{Tx-SN} represents the number of HELLO messages sent by a sensor node and N_{Rx-ON} is the number of ACKs sent by the associated gateway. When the value of LQ is below a certain threshold (LQ_{th}), the sensor node wakes up and starts to broadcasts periodically SOS messages until a gateway answers or a recovery time set a priori is elapsed. If a gateway receives this message it includes the orphan sensor node in its cluster sending a HELP message. At the end of the procedure the respective tables are updated.

If there are no gateways able to support an orphan sensor node (i.e., HELP messages is not received), the network tries to establish an end-to-end path between the sensor node and a remote gateway. In particular, the orphan sensor node broadcasts periodically SOS messages to the sensor nodes in its coverage area. The recursive application of this flooding procedure sets up a sort of ad-hoc network. The orphan sensor node will choose the path with the minimum number of hops.

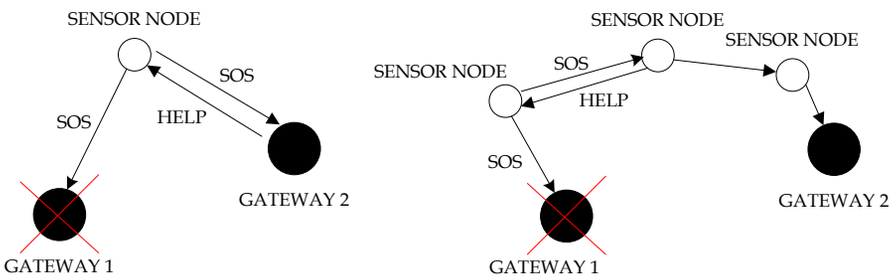

Figure 9. Recovery State

Both the procedures are shown in Fig. 9.

3.2. Application layer

Since higher-level layers and interoperability sub-layers are not defined in the IEEE 802.15.4 standard, a custom protocol was developed to attain a full interaction between the final user and the WSN. The application protocol is composed by:

- CONTROL MESSAGES (i.e., ping, ack), to verify the network status;
- MANAGEMENT MESSAGES, to access part of network element configuration settings and to change some important monitoring parameters;
- DATA MESSAGES, to receive row data from the WSN;
- ERROR MESSAGES, to detect system failures due for example by low battery levels or communication problems.

3.3. Performance analysis

In order to evaluate the performance of the proposed communication protocol in terms of power consumption and latency, some simulations were performed. The simulated system

was developed by means of a network protocol simulator called *NePSing*, that is, a C++ framework specifically designed for modeling the evolution of time-discrete asynchronous networks [20]. Finally, to validate the simulations, the results were compared with those obtained by real measurements.

The most relevant simulation parameters are summarized in Table 2.

Sensor Node	
energy consumption (active mode)	60 mA
energy consumption (sleep mode)	0.7 μA
sleeping sub-period [T_s]	5 s
Ethernet Gateway	
energy consumption (active mode)	60 mA
energy consumption (sleep mode)	1 μA
sleeping sub-period [T_s]	5 s
GPRS Gateway	
energy consumption (active mode)	200 mA
energy consumption (sleep mode)	1 mA
sleeping sub-period [T_s]	5 s

Table 2. Simulation Parameters

The adopted network structure is shown in Fig. 10. It is comprised of a GPRS Gateway, an Ethernet Gateway and twelve sensor nodes deployed in a 50 m x 50 m area.

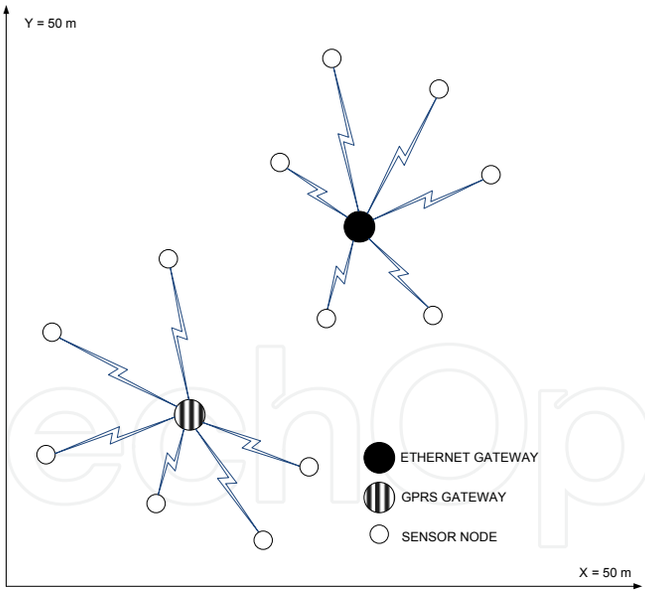

Figure 10. Adopted Network Topology

The adopted antenna model is an ideal smart antenna formed by a group of four non overlapping adjacent beams that cover the omnidirectional area. In particular, an antenna radiates in a fixed sector of $\pi/2$ radians, thus providing an increased gain over a restricted range of azimuths respect to an omnidirectional antenna.

To give an insight on the protocol energy efficiency in Fig. 11 the mean lifetime of the network nodes (sensor nodes, Ethernet Gateway and GPRS Gateway) as a function of sleeping

sub-periods is shown. When the nodes are *always on* ($T_s = 0$), the network lifetime corresponding to the sensor node lifetime is about two days. This time is sufficient to monitor continuously (every 15 s) an art object that is transfered from a museum to another. The introduction of a duty cycle ($T_s \neq 0$) and the use of directive antennas installed on gateways reduce the mean power consumption and increase the mean battery time. For example, the lifetime increment due to the installation of directive antennas on the GPRS Gateway is about 713 days in the case of $T_f = 15\ min$ ($T_s = 895\ s$). Finally, figures highlight the good accurancy of the simulation model by comparing mathematical predictions with real results.

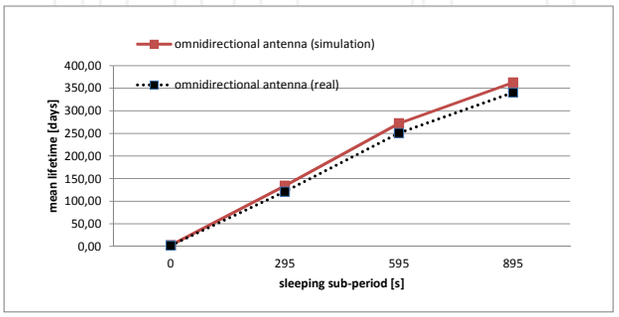

(a) Sensor Node Lifetime

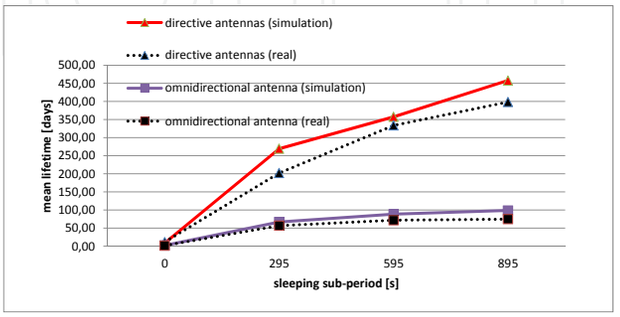

(b) Ethernet Gateway Lifetime

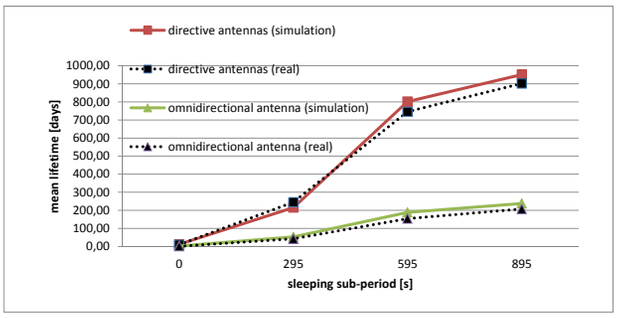

(c) GPRS Gateway Lifetime

Figure 11. Mean Lifetime vs. Sleeping Sub-Period

To conclude the analysis, the mean latency is taken into the account. The mean latency is the time interval between an orphanage detection due to a gateway fault and the consequent sensor node's association with a new gateway. In Fig. 12 the mean latency as a function of the number of sensor nodes is shown. The network nodes are *always on*. The link quality threshold (LQ_{th}) is set to 2. Firstly, it is important to note that the latency is very low thus underlying a low collision probability. It is about 10 s when the deployed sensor nodes are 6. Secondly, the mean latency is a linear function of the number of deployed sensor nodes, thus highlighting a good network scalability.

4. End user interface design

The *Remote Server* stores, processes and presents the information gathered by the WSN. Data are comprised of sensing (measures, battery level) and control/management messages. The final user may check the system status through graphical user interface (GUI) accessible via web. After the log-in phase, the user can select the proper monitored scenario (i.e., a museum,

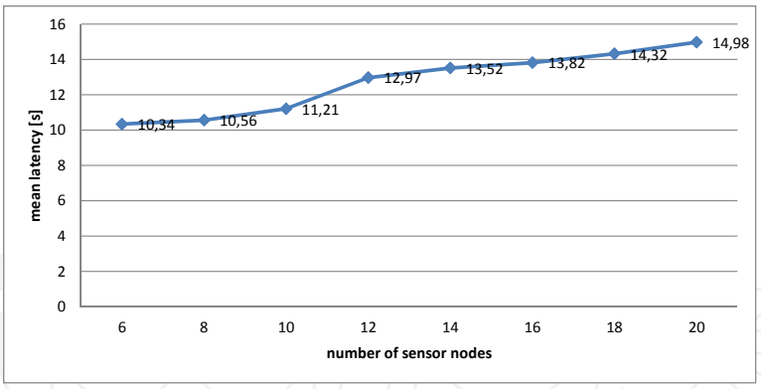

Figure 12. Mean Latency vs. Number of Sensor Nodes

a particular room or a particular art object). For each scenario the deployed WSN together with the gateway or part of WSN is schematically represented through an interactive map. In addition to this, the related sensors display individual or aggregate time diagrams for each node with an adjustable time interval (Start/Stop) for the observation. System monitoring could be performed both at a high level with a user friendly GUI and at a low level by means of message logging.

Afterwards two GUI examples are briefly described.

In Fig. 13 the frequency distribution and the cumulative frequency of the relative humidity are represented. The *frequency distibution* is the number of occurrences of a repeating value of a phenomenon per observation time. The *cumulative frequency* is the frequency of occurrence of values of the phenomenon less than or equal a reference value. For example the figure shows that during the observation period 1410 monitored samples of the relative humidity have assumed values within the interval between 40% - 45%. While 78% of monitored values are less or equal than 45%.

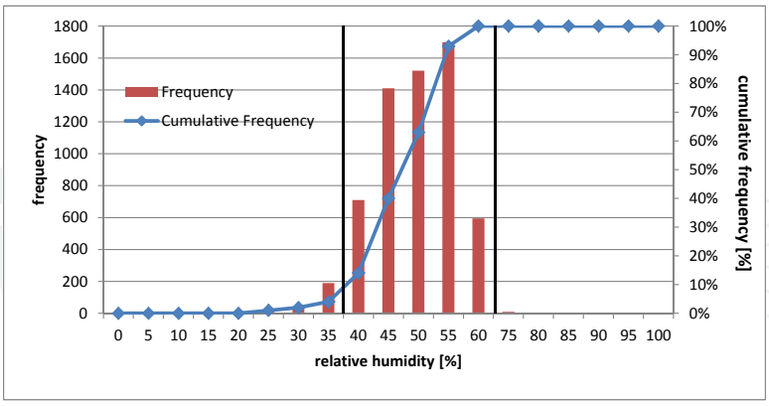

Figure 13. Frequency Distribution and Cumulative Frequency of the Relative Humidity

In Fig. 14 a temperature and relative humidity matrix obtained in 10 observation days and the related global *Performance Index* (PI) are shown. The PI is defined as the percentage of time in which the measured parameter lies within the required (tolerance) range. In this case the tolerance ranges are [40% - 60%] and [19C° - 24C°] for the relative humidity and the temperature respectively. The evaluated PI is 96.3%.

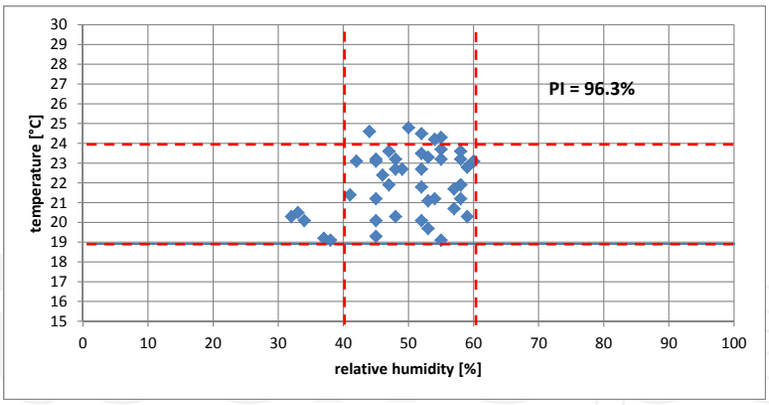

Figure 14. Global Performance Index on Temperature and Relative Humidity Matrix

5. Real experiences

The WSN system described above was tested and deployed in our laboratory and in one pilot site. The collected data represents a database of information on changes of the environmental parameters considered the principal causes of deterioration of art and artifacts.

5.1. System tests

On May 1^{st} 2009 in two rooms of our laboratory the first deployment was performed in order to evaluate the protocol performance and the capability of the system to provide useful and essential informations on changes of the principal environmental parameters. In fact the transition from Spring to Summer represents the most critical phase of the year from the point of view of climatic oscillations.

Eight sensor nodes equipped with temperature-humidity and light sensors and one Ethernet Gateway were installed in strategic points of the rooms.

To give an insight on the protocol efficiency, the Message Delivery Rate (MDR) was evaluated as the ratio between the messages correctly received by the remote server and the expected transmitted messages. After five months each sensor node showed a MDR over 97% in the case of a sampling interval equal to 10 minutes and over 94% in the case of 2 minutes. This confirms the robustness of the network and the reliability of the adopted communications solution. Moreover, the plotting data on the test period gave evidence of the usability and the utility of the proposed system. Fig. 15(a) shows that the environmental temperature of the rooms was too high for the optimal maintenance of art and artifacts. In particular from the end of May the temperature rose till the achievement of $28,6C^{\circ}$ thus exceeding the tolerance threshold. Conversely, the relative humidity values remained for most of the time within the optimal conservation range ($40 \leq RH \leq 60$) as Fig. 13 highlights.

In order to evaluate the accuracy of the temperature sensors (SENSIRION - SHT75), another important test was performed in the climatic chamber of the Microelectronic Laboratory of the University of Florence. To this end, a simple network composed by three sensor nodes and one GPRS Gateway was set up within the chamber. As the Fig. 15(b) shows a mean square error equal to 0.1 was evaluated from the comparison between the values detected by the sensor nodes and the reference temperature. This error is low respect to that obtained during the calibration of the commercial devices.

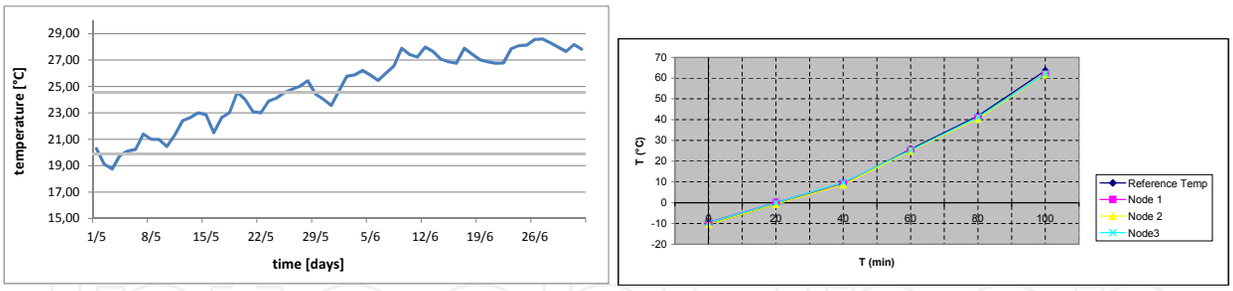

(a) Temperature Time Diagram (b) Climatic Test Chamber

Figure 15. Temperature Tests

In order to evaluate the capability of the system to provide real time informations on the accelerations of moving objects, a road test was performed. Two sensor nodes equipped with one accelerometer-gyroscope sensor were installed inside and outside a container respectively. The container was placed within a van together with a GPRS Gateway.

Fig. 16(a) and Fig. 16(b) show the acceleration values over a fixed threshold, 4.905 m/s^2 for the x and y components and 11.829 m/s^2 for the z component. It is important to note that in the time interval between 11:36 a.m. and 11:47 a.m the container was subjected to considerable ripples caused by a dirt road. The container instead damped the oscillations.

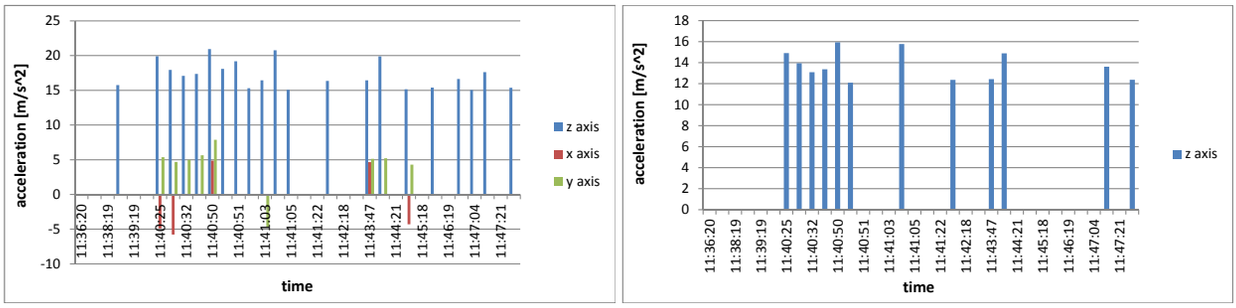

(a) Outside the Container (b) Inside the Container

Figure 16. Acceleration Values

5.2. Pilot site description

The WSN system was deployed to qualify the thermal quality and the presence of gases during a temporary exhibit (paintings) in an Italian museum, throughout the entire heating season (from October to April). The analysis focused on the observation of thermal and hygrometric and gas data. The museum was equipped with two WSNs, controlling both air temperature, relative humidity and carbon dioxide inside and outside the showcases. The exhibit took place on one whole floor of the museum building, across two different exhibit areas. The exhibit floor area was about 1800 m^2 and the average room height was 3.5 m. The rooms were conditioned by an all-air system, working continuously 24 h a day.

The monitoring campaign was performed using 38 sensor nodes (including the gateways) with 107 sensors. These sensor nodes were located in each room, in order to measure and send values every 10 min.

Analysing the thermal quality, a prime importance was given to frequency distribution and cumulated frequency evaluation. Statistical values, frequency distribution, and cumulated frequency are shown, respectively, in Fig. 17(a) and Fig. 17(b). 94% of the relative humidity values are within the required interval of 45-55% (which leads to a PI of 94%), and most of the data are between 49% and 52%. 100% of the temperature values are within the required interval (which leads to a PI of 100%), and most of the data are between 21C° and 22C°.

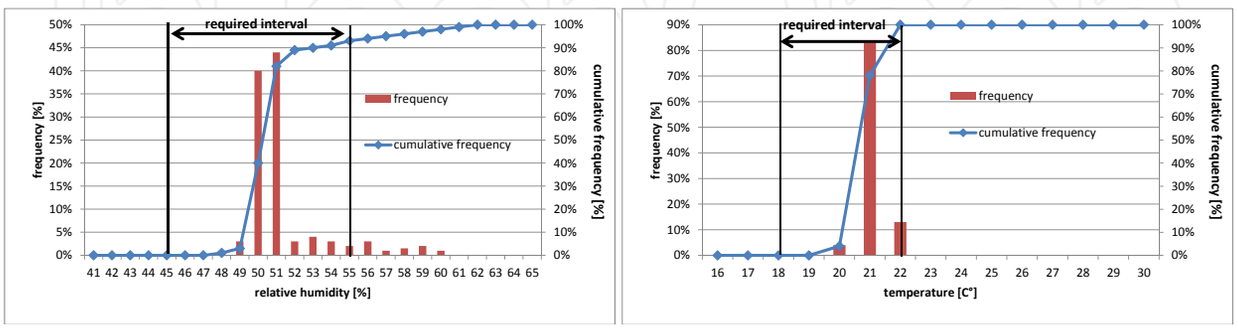

(a) Relative Humidity (b) Temperature

Figure 17. Frequency Distribution and Cumulated Frequency

A new global PI was introduced and calculated, considering both temperature and relative humidity at the same time. It was calculated as the percentage of time in which both temperature and relative humidity are inside the required range. Then the complementary percentage of time referred to the values out of this range was defined, specifying if the Shifted Index (SI) was related to temperature, or relative humidity, or both parameters together. In Fig. 18 even when the PI is higher than 90%, some values shift out of the correct range for preservation. Synthetically, the analysis shows that, considering the whole exhibit area, the PI values are far higher than a "warning value" of 90%, which means 10% of data outside the required ranges.

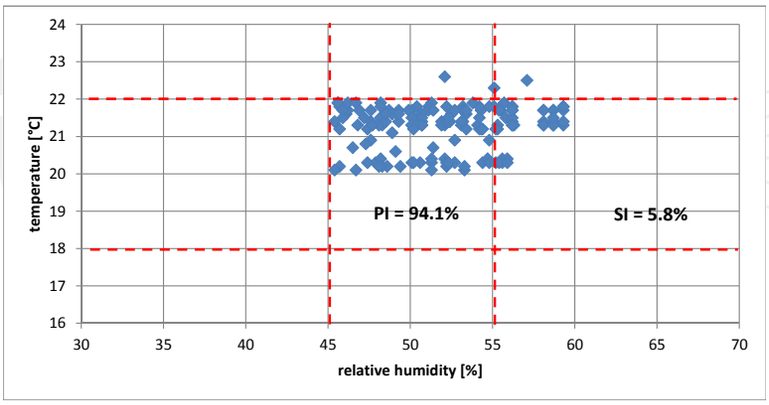

Figure 18. Global Performance Index on Temperature and Relative Humidity Matrix

Another important result regards CO_2 data. In Fig. 19 a temporal diagram of CO_2 behaviour inside and outside the showcases is shown. It is important to note how the showcases protected the artifacts thus reducing the CO_2 emissions under the alert threshold.

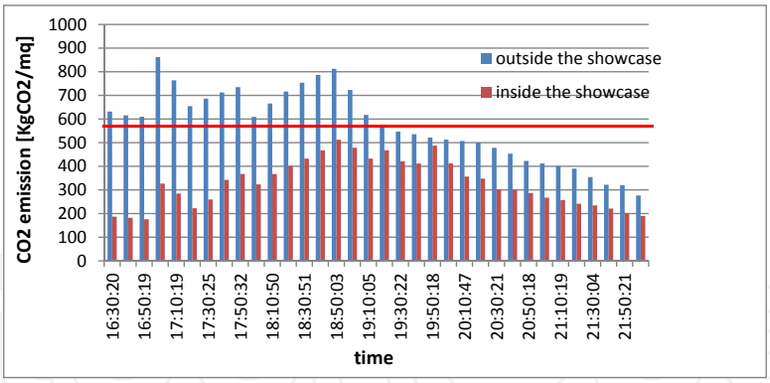

Figure 19. Temporal Diagram of CO_2 Emission

6. Conclusion

This chapter deals with the design, optimization and development of a practical solution for application to the Cultural Heritage monitoring and control. The overall system was addressed in terms of the experiences platform, network issues related both to the node's communication protocol and gateway operations up to the remote user's suitable interface. In particular, the proposed solution was installed in several museums and was used to monitor the art objects during their transport from a museum to another. The experimental results highlighted a noticeable performance as far as the data collecting reliability, the system robustness and the usability are involved. This allows the application of the solution under investigation to the more general field of environmental monitoring, due to its flexibility, scalability, adaptability and self-reconfigurability.

Acknowledgement

The authors would like to thank T.T. Tecnosistemi S.p.A.

Author details

Luca Bencini
T.T. Tecnosistemi S.p.A., Via Rimini 5, 59100 Prato, Italy

Stefano Maddio
Dept. of Electronics and Telecommunication, University of Florence, Via di Santa Marta 3, 50139 Florence, Italy

7. References

[1] Akyildiz, I.F.; Su, W.; Sankarasubramaniam, Y. & Cayirci, E. (2001). Wireless sensor networks: a survey, In: *Journal on Computer Network*, Vol. 38, pp. 393-422, December 2001.

[2] Yick, J.; Mukherjee, B. & Ghosal, D. (2008). Wireless sensor network survey, In: *Journal on Computer Network*, Vol. 52, pp. 2292-2330, April 2008.

[3] Sohraby, K.; Minoli, D. & Znat, T. (2007). Wireless Sensor Networks. Technology, Protocols and Applications, In: *John Wiley & Sons*, 2007.

[4] Karl, H. & Willing, A. (2005). Protocols and Architectures for Wireless Sensor Networks, In: *John Wiley & Sons*, 2005.
[5] Akyildiz, I.F.; Su, W.; Sankarasubramaniam, Y. & Cayirci, E. (2002). A Survey on Sensor Networks, In: *IEEE Communications Magazine*, Vol.40, pp. 102-114, August 2002.
[6] Al-Karaki, J.N. & Kamal, A.E. (2004). Routing Techniques in Wireless Sensor Networks: a Survey, In: *IEEE Communication Magazine*, Vol. 6, pp. 6-28, 2004.
[7] SENSIRION - SHT75. [Online: `http://www.sensirion.com`].
[8] MicroSemi - TAOS TSL252R-LF. [Online: `http://www.microsemi.com`].
[9] City Tech - EZT3NDH, EZT3SH, O33E1F. [Online: `http://www.citytech.com`].
[10] XSens - Mti. [Online: `http://www.xsens.com`].
[11] AK-NORD - XT-Nano-XXL Ethernet Module. [Online: `http://www.ak-nord.de`].
[12] Maddio, S., Cidronali, A. & Manes, G. (2011). A new design method for single-feed circular polarization microstrip antenna with an arbitrary impedance matching condition, In: *IEEE Transactions on Antennas and Propagation 59*, pp. 379-389, January 2011.
[13] Cidronali, A., Maddio, S., Giorgetti, G. & Manes, G. (2010). Analysis and performance of a smart antenna for 2.45-ghz single-anchor indoor positioning, In: *IEEE Transactions on Microwave Theory and Techniques, IEEE Transactions on 58*, pp. 21-31, January 2010.
[14] Sveda, M.; Benes, P; Vrba, R. & Zezulka, F. (2005). Introduction to Industrial Sensor Networking, In: *Handbook of Sensor Networks: Compact Wireless and Wired Sensing Systems*, pp. 10-24, 2005.
[15] Shakkottai, S.; Rappaport, T.S. & Karlsson, P.C. (2003). Cross-layer Design for Wireless Networks, In: *IEEE Communication Magazine*, Vol. 41, pp. 74-80, October 2003.
[16] Jain, J.N. & Agrawala, A.K. (1992). Open Systems Interconnection: Its Architecture and Protocols, In: *Mcgraw-Hill Series on Computer Communications*, November 1992.
[17] Wireless Medium Access Control (MAC) and Physical Layer (PHY) Specifications for Low-Rate Wireless Personal Area Networks (LR-WPANs), In: *IEEE Standard 802.15.4*, 2003.
[18] Ye, W.; Heidemann, J. & Estrin, D. (2002). An Energy-Efficient MAC Protocol for Wireless Sensor Networks, In: *Proc. of INFOCOM 2002*, Vol. 3, pp. 1567-1576, June 2002.
[19] Dam, T. & Langendoen, K. (2003). An Adaptive Energy-Efficient MAC Protocol for Wireless Sensor Networks, In: *Proc. of SENSYS 2003*, pp. 171-180, November 2003.
[20] Pecorella, T. NePSing - Network Protocol Simulator ng. [Online: `http://nepsing.sourceforge.net`].